Effects of Material Degradation on the Structural Integrity of Composite Materials: Experimental Investigation and Modeling of High Temperature Degradation Mechanisms

FINAL REPORT for
Grant NAG3-1760

Submitted to:

NASA Lewis Research Center
Attn: C. Chamis and D. Bowles
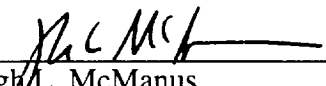21000 Brookpark Road
Cleveland, OH 44135

March 1996

by

Ronan A. Cunningham, Research Assistant, S.M. Candidate, and
Hugh L. McManus, Class of 1943 Career Development Assistant Professor

TECHNOLOGY LABORATORY FOR ADVANCED COMPOSITES
Department of Aeronautics and Astronautics
Massachusetts Institute of Technology
Cambridge, Massachusetts 02139

Principal Investigator:_____

Hugh L. McManus
Class of 1943 Assistant Professor of
Aeronautics and Astronautics

1

EXPERIMENTAL INVESTIGATION AND MODELING OF HIGH TEMPERATURE DEGRADATION MECHANISMS

Ronan A. Cunningham[1] and Hugh L. McManus[2]
Technology Laboratory for Advanced Composites
Department of Aeronautics and Astronautics
Massachusetts Institute of Technology
Cambridge, MA 02139

It has previously been demonstrated that simple coupled reaction-diffusion models can approximate the aging behavior of PMR-15 resin subjected to different oxidative environments [1]. Based on empirically observed phenomena [2-7], a model coupling chemical reactions, both thermal and oxidative, with diffusion of oxygen into the material bulk should allow simulation of the aging process. Through preliminary modeling techniques such as this it has become apparent that accurate analytical models cannot be created until the phenomena which cause the aging of these materials are quantified. An experimental program is currently underway to quantify all of the reaction/diffusion related mechanisms involved. The following contains a summary of the experimental data which has been collected through thermogravimetric analyses of neat PMR-15 resin, along with analytical predictions from models based on the empirical data.

Thermogravimetric analyses were carried out in a number of different environments - nitrogen, air and oxygen. The nitrogen provides data for the purely thermal degradation mechanisms while those in air provide data for the coupled oxidative-thermal process. The intent here is to effectively subtract the nitrogen atmosphere data (assumed to represent only thermal reactions) from the air and oxygen atmosphere data to back-figure the purely oxidative reactions. Once purely oxidative (concentration dependent) reactions have been quantified it should then be possible to quantify the diffusion of oxygen into the material bulk.

The thermogravimetric analyses in nitrogen were carried out at three different heating rates - 10°C/min, 15°C/min and 20°C/min. Data was obtained from three different PMR-15 resin plaques and is presented in the Figures 1-6. The data shown here has been normalized, with a normalized weight loss equal to 1 representing a total weight loss of approximately 40% of the original specimen. As can be seen in the figures, the data is quite clean and demonstrates good consistency. A variety of different forms of neat resin were also tested, from coarse granules, to shavings, to sieved powders. No noticeable discrepancy in the location and magnitudes of the peaks was observed, confirming that this is in fact a bulk mechanism. This is not the case for tests carried out in air, however, due to the diffusion related dependency which is involved. In all cases, the weight loss rate of the material contains two distinct peaks. Typically, if a single reaction is responsible for the degradation of the material (which is represented by a loss of mass) then only one peak will be visible. The presence of a second peak in this case suggests the presence of two, simultaneously occurring, reactions. This correlates with other empirical observations which suggest that the mass loss due to aging is in fact attributed to the degradation of separate components of the resin. In particular, it has been suggested by Alston [8] that approximately 2/3 of mass loss can be attributed to the degradation of unreacted endgroups, while the remaining 1/3 is potentially from the degradation of polymerized endgroups.

---

[1]Research Assistant, S.M. Candidate
[2]Class of 1943 Career Development Assistant Professor

The model which is proposed here to simulate the thermal degradation of the material uses two Arrhenius reactions. Each of these reactions acts on a different material component (unreacted or polymerized endgroups) and are in effect decoupled from one another. The basic equations for the Arrhenius reactions (placing no assumptions on the order of the reactions) can be represented as follows:

$$\frac{d\alpha_1}{dt} = k_1(1-\alpha_1)^n exp\left(\frac{-E_1}{RT}\right)$$

$$\frac{d\alpha_2}{dt} = k_2(1-\alpha_2)^m exp\left(\frac{-E_2}{RT}\right) \tag{1}$$

$$\frac{d\alpha_{total}}{dt} = y_1\frac{d\alpha_1}{dt} + y_2\frac{d\alpha_2}{dt}$$

These equations only apply to the thermal cases where there is no concentration dependency involved in the reactions. The variables α_1 and α_2 represent the normalized weight loss of the material components, with $\alpha=1$ when the reaction has completed. E_1 and E_2 are the activation energies, k_1 and k_2 are the reaction constants and y_1 and y_2 are the fractions of the overall weight loss which are accounted for by each individual degradation mechanism. The only assumption made here is that $y_1 = 0.33$ and $y_2 = 0.67$, as per Alston's observations. The determination of the appropriate coefficients is complicated by the close coupling between the activation energy and reaction constant is each of the reactions. There is no simple relationship whereby changing, say, the activation energy only affects the position of the peak or changing the reaction constant only affects the magnitude of the peak. Instead, the changing of either of these variables will affect both the location and magnitude of the peak. The Kissinger method was used to reduce the data whereby the temperature of the peak in the weight loss rate curve, T_{max}, is related to the heating rate, q, by

$$\ln\left(\frac{q}{T_{max}^2}\right) = \ln\left(\frac{kR}{E}n(1-\alpha)^{n-1}\right) - \frac{E}{RT_{max}} \tag{2}$$

A plot of $\ln(q/T^2)$ as a function of ($1/T$) allows the activation energy to be found from the slope and the reaction constant, k, can be found from the intercept if the order of the reaction (n or m) is known. An expression for the order of the equation can be found by solving for k from the intercept and substituting it into (1), viz.

$$n = \left(\frac{d\alpha}{dt}\right)^{-1}\frac{EB}{R}(1-\alpha)exp\left(\frac{-E}{RT}\right) \tag{3}$$

where $B=\exp($intercept value$)$. This approach requires values for $d\alpha/dT$ and α, as well as q and T at the maximum weight loss rate. Using this approach, and the thermal data which has been collected, it was possible to obtain the necessary six reaction constants. These constants are shown in Table 1. Even though the reactions act separately, there is a strong interaction between them in terms of the overall weight loss. Figure 7 shows the individual reactions and their combined effect. It can be seen from this that the peaks of the overall mechanism are results of both reactions, with the individual peaks being located slightly to the left or right of the combined peak locations. While this complicated the reduction procedure it was still possible to obtain reasonable coefficients which simulate the behavior across the three heating rates. Figures 8-10 compare the model predictions with the empirical data at different heating rates. In all cases the agreement is very good. Table 2 compares the peak locations and peak magnitudes of

3

the model to those of the data. The model is capable of predicting quite accurately the shifts in locations and changes in magnitude of the peaks across the various heating rates, suggesting that the correct mechanics have been trapped.

It is worth making a few comments at this stage about the reactions depicted in Figure 7. The overall mechanism is quite clearly a combination of two individual reactions, which interact with one another only in an additive fashion. However, these reactions are significant in two different temperature zones. As we can see the first reaction peaks at a temperature around 500°C, while the second does not peak until approximately 570°C. The overall effect of this is that the weight loss in the temperature region 300°C-400°C will almost exclusively be due to the first reaction only, with the second reaction not really being activated until we reach temperatures in excess of 400°C. At temperatures below 300°C, the reactions are progressing but at a rate so slow many hundreds of hours of exposure are required before a noticeable weight loss can be recorded. Previous investigations [3] have recorded significant weight loss in PMR-15 bulk specimens after only a couple of hundred hours, in air, at temperatures in the region of 300°C. Isothermal aging temperatures of 288°C, 316°C and 343°C were used over periods of several thousand hours. In particular, the weight loss at 343°C was so large, and the damage to the specimen so extensive, after approximately 500 hours that the sample measurements were terminated at that point. This kind of behavior can not be explained in terms of the thermal reactions only. A clearer picture of what is occurring at these test temperatures can be formed by looking at the thermogravimetric analyses of PMR-15 powder in air.

Figure 11 shows a typical plot for the weight loss rate of PMR-15 in air at a heating rate of 20°C/min, along with the data obtained for the purely thermal case. Several differences can be noticed between the thermal and oxidative cases. The first of these is that a peak occurs at a temperature much lower than that found for either of the thermal peaks. This peak suggests the presence of a third reaction which is activated at much lower temperatures than the thermal reactions. Note that the weight loss rate is significant from 300°C upwards. This correlates well with the rapid increase in weight observed as the temperature for isothermal tests is increased from 288°C to 343°C. In fact, by 343°C the oxidative reaction is progressing so fast that any material exposed to the atmosphere will begin to disintegrate very rapidly indeed. The second point to notice is that the magnitude of the peak in air at the location of the first thermal peak is considerably lower than in nitrogen. This would suggest that the oxidative reaction is acting upon the same material, robbing the thermal reaction of raw material before it can begin. Also, the total weight loss found in these experiments equals the original mass of the specimen, i.e. the material is completely digested in the presence of oxygen. Hence, a normalized weight loss equal to 1 will mean that no material is present any longer. The constant weight loss rate at temperatures above 700°C is most likely an ablative process where the remaining charred material is being burnt away.

Efforts are concentrated at the moment on developing models which can simulate the combined oxidative-thermal mechanism. Reduction procedures have as yet not produced reliable kinetic constants for the oxidative process. The modeling of this process is considerably more complicated than in the thermal case as we now have at least one concentration-dependent reaction which acts on the same material as the thermal reactions. Probably there are several such reactions. This results in a much larger number of coefficients which must be determined. Currently, additional thermogravimetric analyses are being carried out on the material, in both air and pure oxygen, in order to provide a more extensive database on the material behavior under these conditions. This should allow reliable models to be developed for the remaining unknown reactions.

Once models for the oxidative components of the weight loss have been determined, work will then concentrate on determining accurate diffusion coefficients for the material. As the kinetic constants for oxygen-dependent reactions will be known, the diffusion rate of oxygen into the

4

material bulk can be determined by visual observation of the growth of surface layers on macroscopic specimens and from the corresponding mass loss. By coupling the resulting diffusion and reaction kinetics a predictive analytical model for the degradation state of the material can be developed.

The thermogravimetric analyses have proven invaluable so far in gaining a true insight to the degradation mechanisms which occur in a material. Seemingly simple weight loss mechanisms have proven in fact to be highly coupled and complicated, with many reactions ongoing simultaneously, albeit with varying relative importance depending on the temperature range being considered. In particular, the analyses have provided a good explanation for the rapid weight loss observed in oxidative aging and why this phenomenon changes so significantly as temperature is increased. Perhaps the most significant result from these analyses is the ability to identify where mechanisms change over, with one dominating the other or vice versa. By understanding the relative influence of these reactions it should be possible to design accelerated aging tests which remain within the regime found at the service temperature, ensuring that the correct mechanism is activated and scaling of results can be performed. This capability is exceptionally important when we are considering the long service lifetimes that components made from these materials are expected to endure.

The immediate work which will be carried out is the conclusion of the thermogravimetric analyses on the PMR-15 powder and the reduction of this data to a form which is amenable to the modeling techniques employed so far. This will then be closely followed by the commencement of tests on macroscopic PMR-15 resin and composite specimens in order to determine the correct diffusion coefficients.

REFERENCES

1. McManus, H.L., and Cunningham, R.A., "Coupled Materials and Mechanics Analyses of Durability Tests for High Temperature Polymer Matrix Composites", presented at ASTM Second Symposium on High Temperature and Environmental Effects on Polymeric Composites, Norfolk, VA, November 1995.

2. Bowles, K.J., "Thermo-Oxidative Stability Studies of PMR-15 Polymer Matrix Composites Reinforced with Various Continuous Fibers", *SAMPE Quarterly*, Vol. 21, No. 4, 1990, pp. 6-13.

3. Bowles, K.J., Jayne, D.,, and Leonhardt, T.A., "Isothermal Aging Effects on PMR-15 Resin", *SAMPE Quarterly*, Vol. 24, No. 2, 1993, pp. 3-9.

4. Bowles, K.J., and Nowak, G., "Thermo-Oxidative Stability Studies of Celion 6000/PMR-15 Unidirectional Composites, PMR-15, and Celion 6000 Fiber", *Journal of Composite Materials*, Vol. 22, 1988, pp. 966-985

5. Alston, W.B., "Resin/Fiber Thermo-Oxidative Interactions in PMR-Polyimide/Graphite Composites", Proceedings of Twenty-Fourth National SAMPE Symposium, San Francisco, CA, May, 1979.

6. Nam, J.D., and Seferis, J.C., "Anisotropic Thermo-Oxidative Stability of Carbon-Fiber Reinforced Polymeric Composites", *SAMPE Quarterly*, Vol. 24, No. 1, October 1992, pp. 10-18

7. Bowles, K.J., Jayne D., Leonhardt, T.A., and Bors, D., "Thermal Stability Relationships Between PMR-15 and Its Composites", *Journal of Advanced Materials*, Vol. 26, No.1, October 1994, pp. 23-32.

8. Alston, W.B., Gluyas, R.E., and Snyder, W.J., "Cyclopentadiene Evolution During Pyrolysis-Gas Chromatography of PMR Polyimides", Proceedings of the Fourth International Conference on Polyimides, Ellenville, NY, October 30-November 1, 1991.

Table 1 - Kinetic constants for thermal reactions

E_1 (J/mol)	169.05×10^3
E_2 (J/mol)	209.22×10^3
k_1 (min^{-1})	2.536×10^{11}
k_2 (min^{-1})	6.07×10^{12}
n	1.29
m	2.63
y_1	0.33
y_2	0.67

Table 2 - Peak locations and peak magnitudes

	Empirical Data		Model	
	Location (°C)	Magnitude	Location (°C)	Magnitude
Peak 1 - q = 10°C/min	493	0.049	482	0.052
Peak 2 - q = 10°C/min	550	0.055	548	0.056
Peak 1 - q = 15°C/min	495	0.075	494	0.077
Peak 2 - q = 15°C/min	561	0.079	558	0.083
Peak 1 - q = 20°C/min	502	0.103	503	0.102
Peak 2 - q = 20°C/min	564	0.106	565	0.109
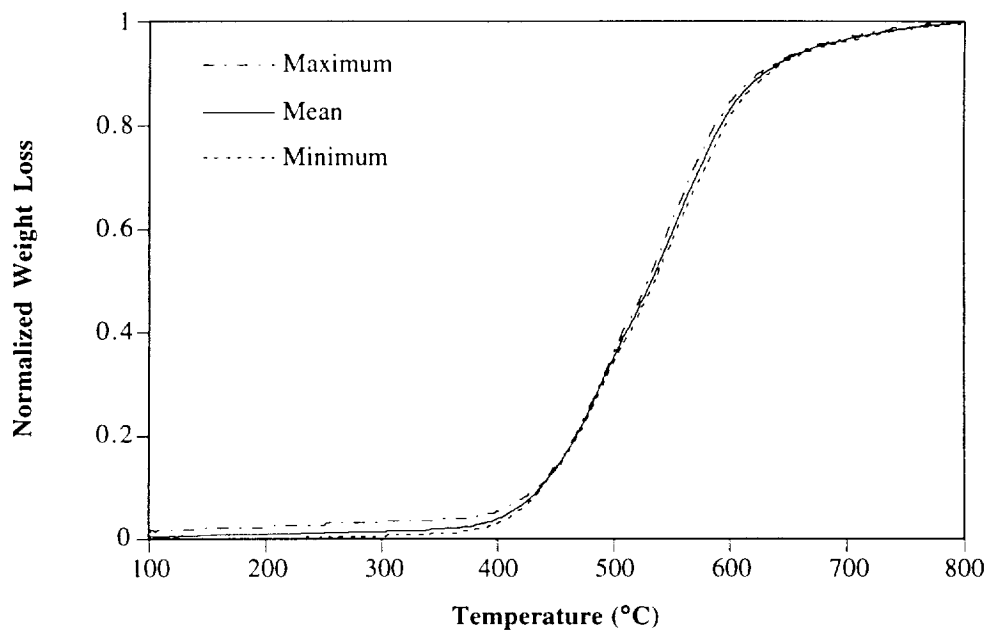
Figure 1.   Normalized weight loss for heating rate 10°C/min
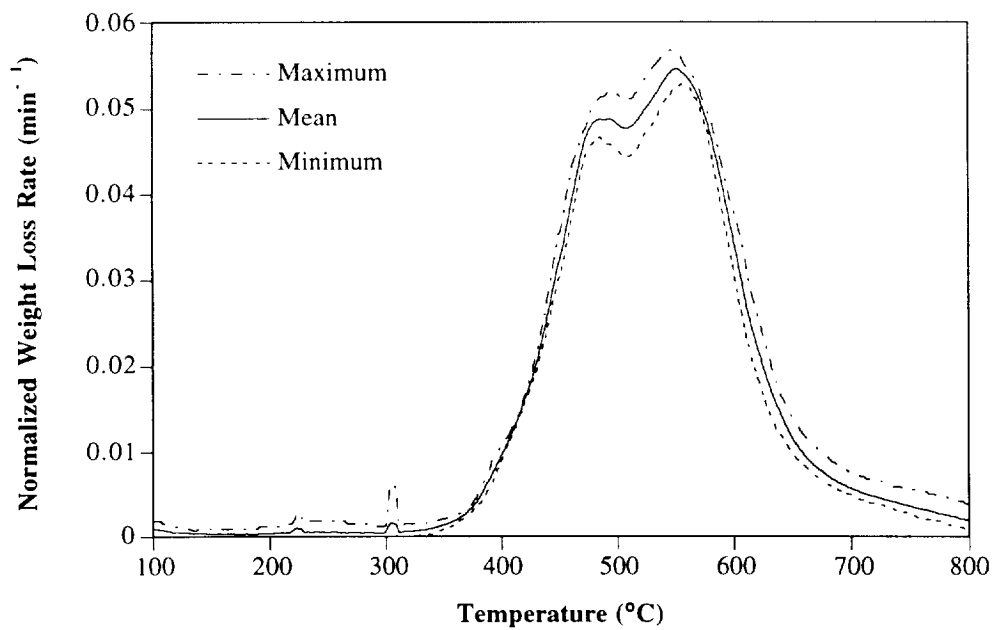
Figure 2.   Normalized weight loss rate for heating rate 10°C/min
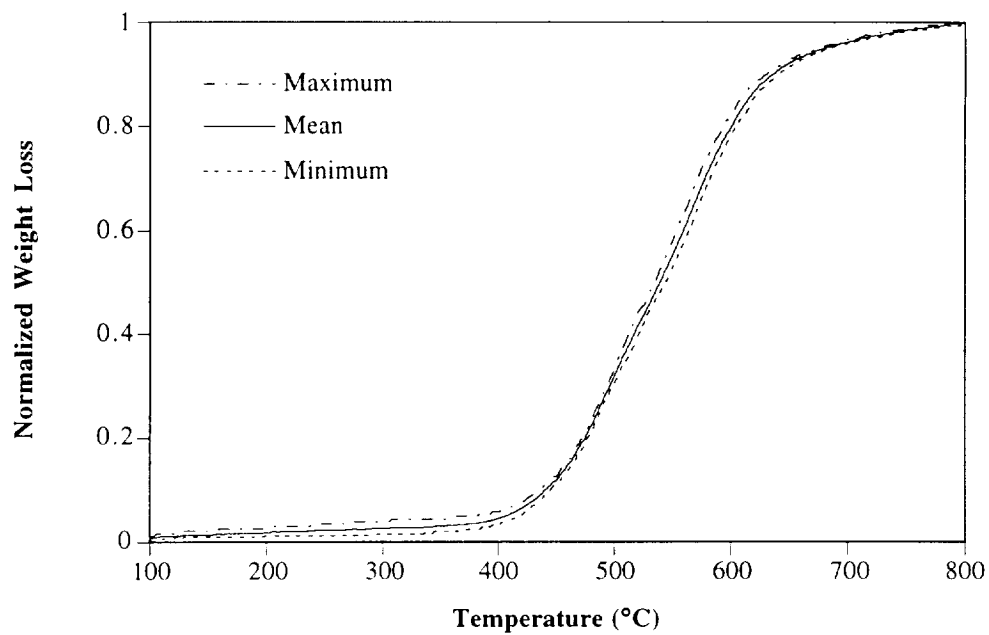
Figure 3.   Normalized weight loss for heating rate 15°C/min
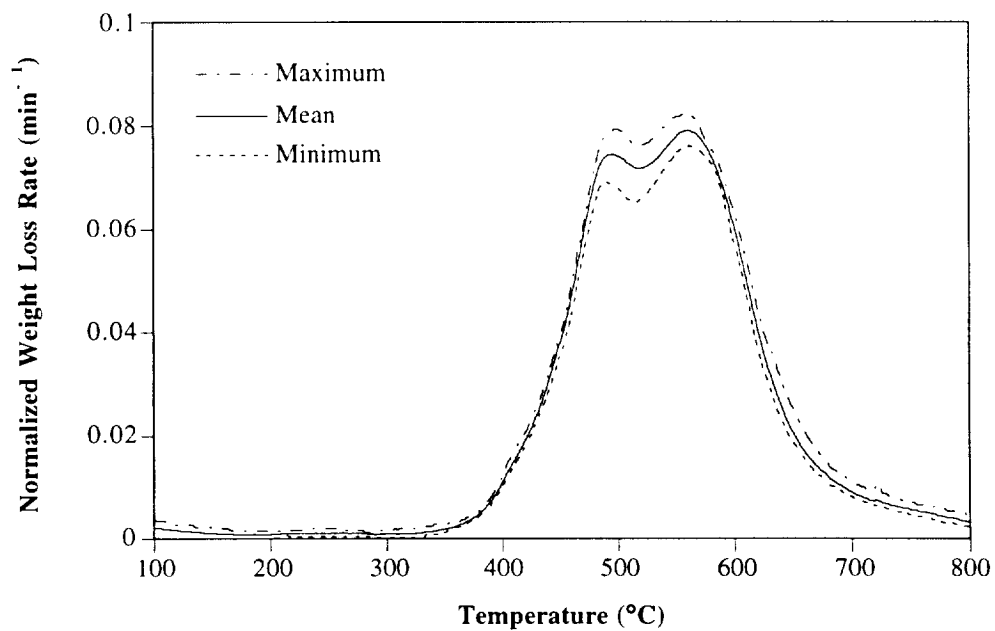
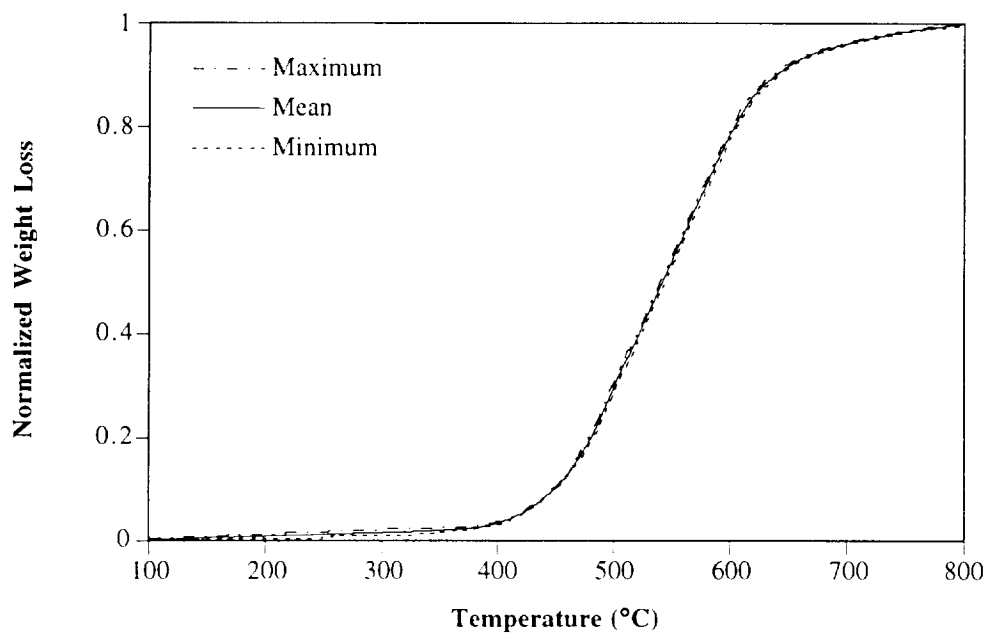Figure 4.   Normalized weight loss rate for heating rate 15°C/min

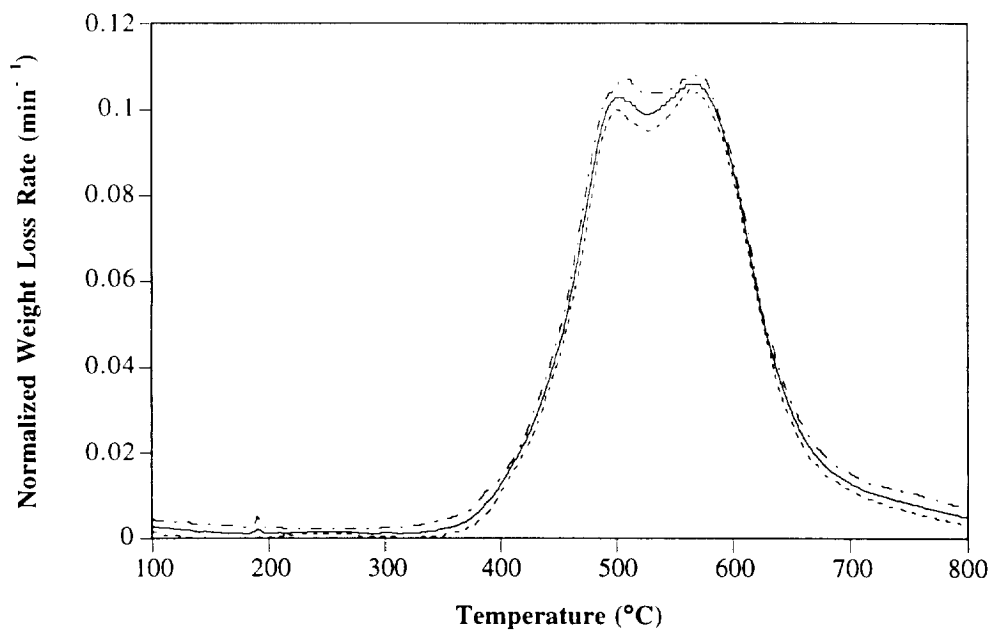Figure 5.   Normalized weight loss for heating rate 20°C/min

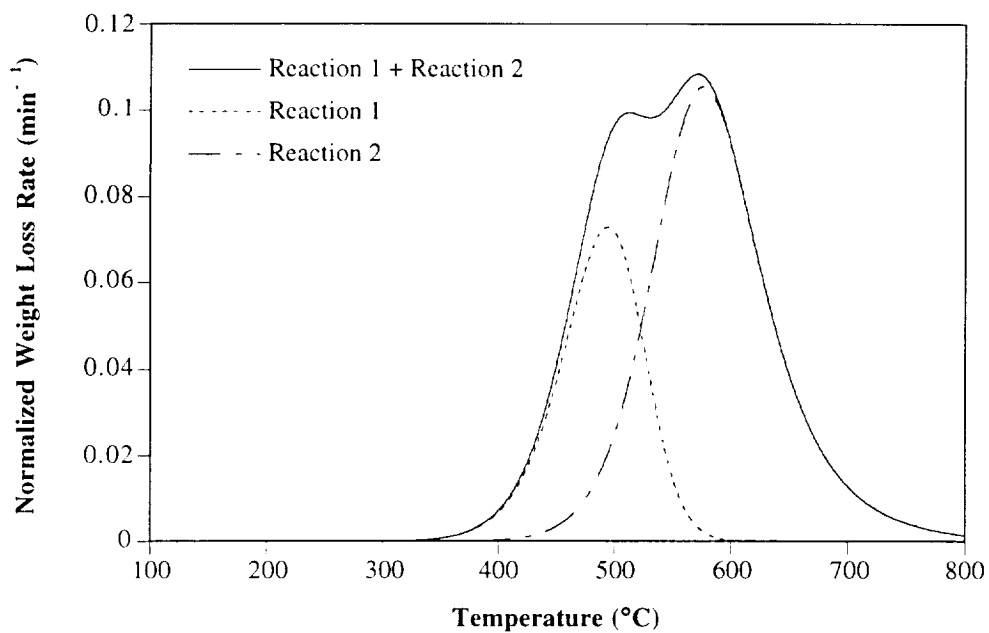Figure 6.   Normalized weight loss rate for heating rate 20°C/min
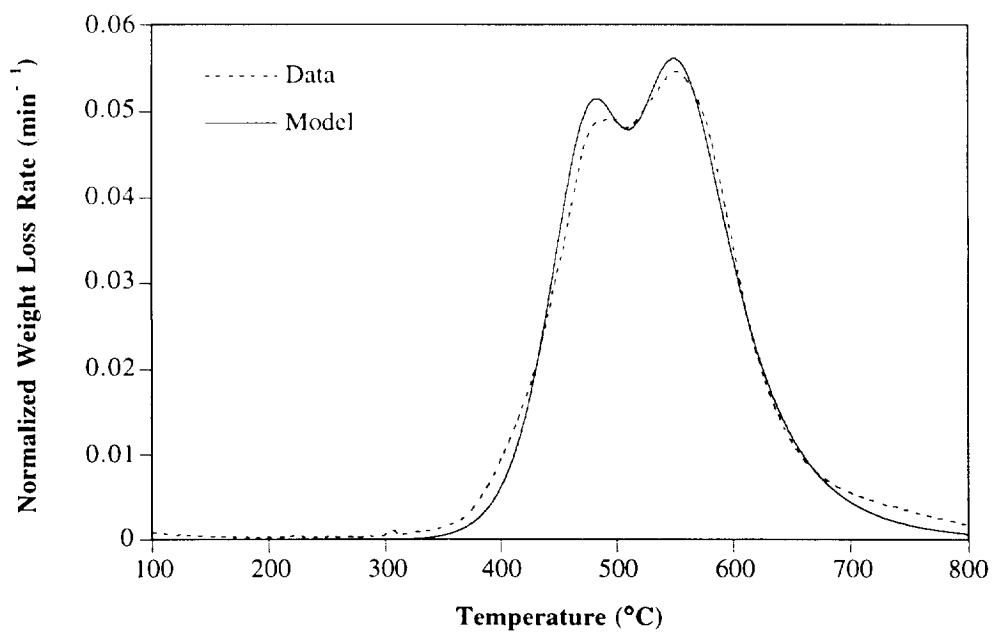
10

Figure 7.   Individual reactions and combined effect
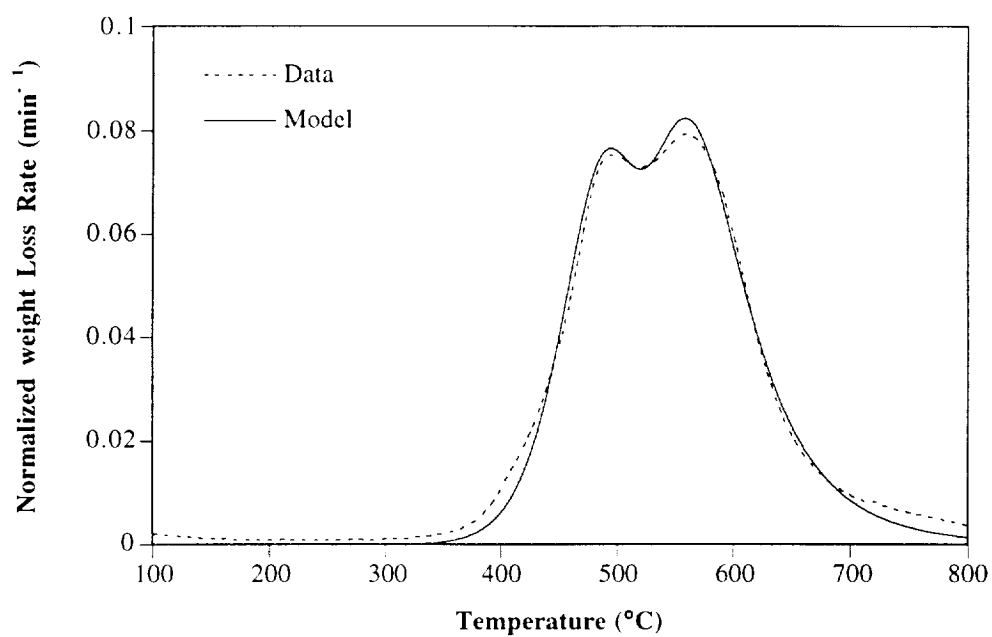

Figure 8.   Model vs data for heating rate 10°C/min

Figure 9.   Model vs data for heating rate 15°C/min
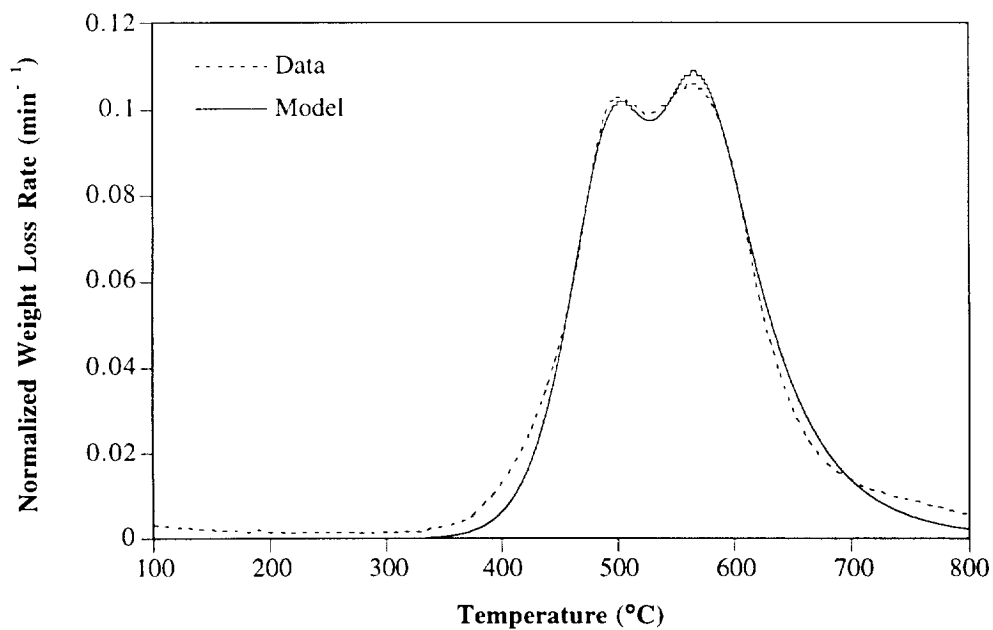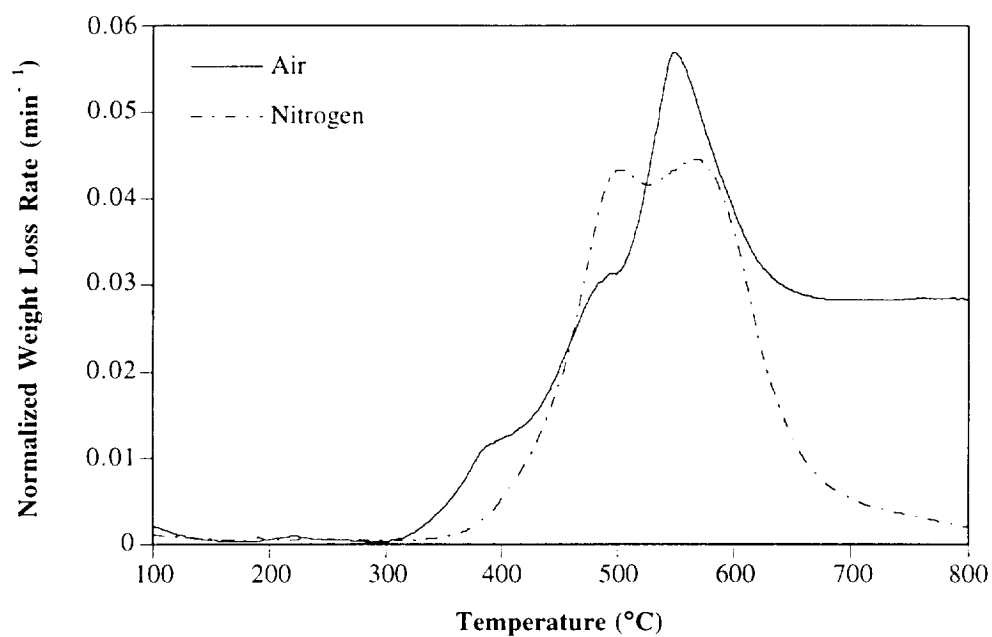
Figure 10.   Model vs data for heating rate 20°C/min

Figure 11. Normalized weight loss rate in air and nitrogen for heating rate 20°C/min